Journal of the European Ceramic Society 7 (1991) 101–108

SiC Whiskers Reinforced Si_3N_4 Matrix Composites: Oxidation Behaviour and Mechanical Properties

J. M. Desmarres, P. Goursat, J. L. Besson

Laboratoire de Céramiques Nouvelles, URA, CNRS 320, Limoges, France

P. Lespade & B. Capdepuy

Aérospatiale, St Médard en Jalles, France

(Received 16 July 1990; revised version received 9 October 1990; accepted 22 October 1990)

Abstract

Different grades of silicon nitride based composites are prepared by hot pressing: $SiC_w/SiAlYON$, SiC_w/Si_3N_4–MgO. The whisker content varies from 0 to 30 wt%. Oxidation in air is studied in the 1350–1500°C temperature range. The same oxidation mechanisms as for the monolithic counterparts are observed. The kinetics depend on the amount and on the composition of the intergranular phase. The mechanical strength and creep resistance are compared with those of the non-reinforced materials. The presence of whiskers enhances the modulus of rupture at high temperature. The creep deformation diminishes as the whisker content increases. The modification of the degradation mechanisms is explained by the hindrance of grain boundary sliding.

Auf Si_3N_4-Basis wurden durch Heißpressen folgende Verbundwerkstoffe hergestellt: SiC_w/Si_3N_4–MgO und $SiC_w/SiAlYON$. Der Anteil an nadelförmigen Kristallen (Whisker) wurde zwischen 0–30 Gew.% variiert. Das Oxidationsverhalten in Luft wurde im Temperaturbereich von 1350°C bis 1500°C untersucht. Man beobachtet die selben Oxidationsmechanismen wie im Falle der entsprechenden keramischen Werkstoffe ohne Whiskerzugabe. Die Kinetik der Oxidation hängt von der Menge und der Zusammensetzung der intergranularen Phase ab. Die mechanische Festigkeit und das Kriechverhalten dieser Werkstoffe wurden mit denjenigen der unverstärkten Werkstoffe verglichen. Durch die Whiskerzugabe verbessert sich sowohl die Hochtemperaturfestigkeit als auch das Kriechverhalten. Diese erhöhte Hochtemperaturfestigkeit wird dadurch erklärt, daß die Whisker das Korngrenzengleiten verhindern.

Différentes nuances de composites à matrice nitrure de silicium ont été élaborées par frittage sous charge: $SiC_f/SiAlYON$, SiC_f/Si_3N_4–MgO. La teneur en trichites varie de 0 à 30% en poids. Le comportement à l'oxydation dans l'air a été étudié dans l'intervalle de température 1350–1500°C. On observe les mêmes mécanismes d'oxydation que pour les monolithiques. Les cinétiques dépendent de la quantité et de la composition des phases intergranulaires. La résistance mécanique et la tenue au fluage sont comparées à celles des matériaux non renforcés. La présence des trichites améliore la tenue mécanique à chaud. La déformation au fluage diminue lorsque la teneur en trichites augmente. La modification des mécanismes s'explique par le fait que les trichites entravent les glissements aux joints de grains.

1 Introduction

The studies on short fibre reinforced ceramic composites have long been delayed because of the thermal instability of the available fibres. The development of processes allowing the elaboration of high-performance whiskers has given rise to a renewed interest for this class of materials.[1,2]

The system SiC whiskers–Si_3N_4-based matrix has been selected due to the chemical compatibility of SiC and Si_3N_4 at high temperature[3] and their high

Journal of the European Ceramic Society 0955-2219/91/$3.50

intrinsic properties. The highly covalent nature of the Si–N bonds inhibits the densification which necessitates the use of additives, usually oxides (MgO, Al_2O_3, Y_2O_3). Densification occurs by liquid-phase sintering. After cooling the thermodynamic equilibrium is not reached. An intergranular vitreous phase remains in the structure, which controls the behaviour of the material at high temperature.

This study concerns the oxidation resistance and the mechanical properties of these composites. The role of the whiskers content, the influence of the microstructure of the matrix and especially the nature of the intergranular phases are investigated.

2 Materials

2.1 Starting materials

The silicon carbide whiskers (β-SiC, ϕ ranging from 0·2 to 1 μm; Tateho Chemical Industries, Japan) contain oxygen and metallic impurities (Al, Mg, Ca, Fe). The SiAlYON (Céramiques et Composites, France) is obtained by nitridation of silicon (impurities Ca, 0·14 wt%; Fe, 0·54 wt%) and aluminium (5·6 wt%) powders mixed with yttria (14 wt%). The phases determined by X-ray analysis are the β'-$Si_{6-z}Al_zO_zN_{8-z}$ ($z = 0{\cdot}8$) solid solution as the major compound together with oxynitride $YSiO_2N$ and yttrium silicate ($Y_2Si_2O_7$) in low quantities. The compacts are ground. The resulting mean particle size is about 1·5 μm. The silicon nitride powder (SNE10 UBE Industries, Japan) has a mean particle size of 0·6 μm and contains 2 wt% oxygen and C, Cl, Ca, Al as impurities.

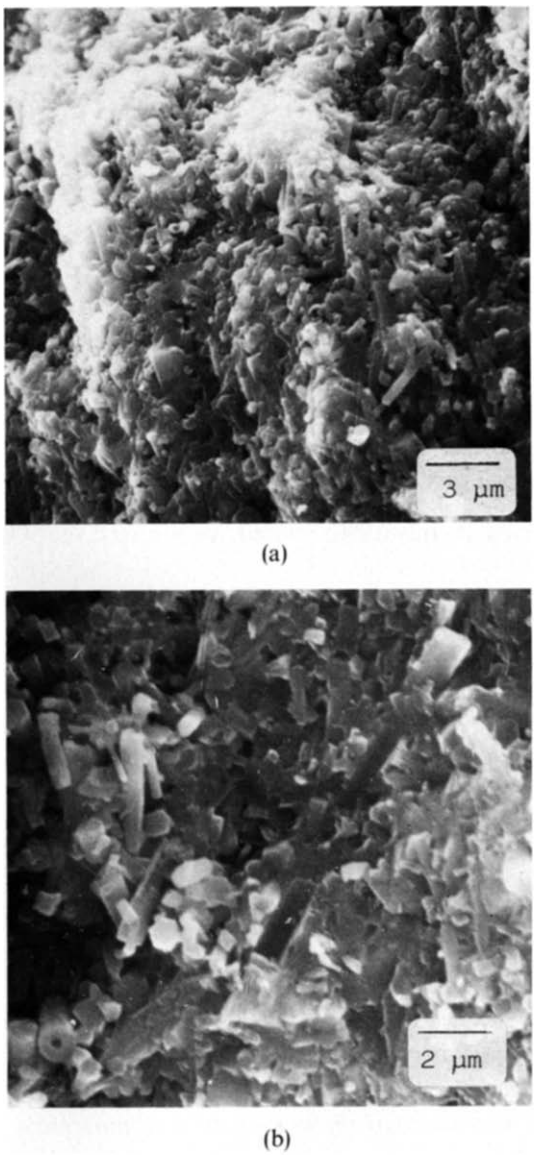

Fig. 1. SEM: Rupture surfaces. (a) SiC_w/SiAlYON; (b) SiC_w/Si_3N_4–MgO.

2.2 Elaboration

Short fibre composites can be fabricated following different routes. However an homogeneous distribution of whiskers in the matrix is always difficult to achieve. The mixing of the powders is achieved in a liquid medium. The process route includes three main stages: (i) the powders (Si_3N_4–MgO or SiAlYON) and the whiskers are mixed in alcohol with a dispersent agent, (ii) the slip is energetically stirred and filtered under gas pressure, (iii) the bodies are hot pressed in nitrogen in the 1650–1750°C temperature interval with pressures ranging from 20 to 40 MPa. The same method is used for composites with the sialon-based matrix and the Si_3N_4–4 wt% MgO matrix. The experimental details are described elsewhere.[4] For each series two grades of composites are made: 15 or 30 wt% SiC whiskers. The porosity is less than 5% for all the discs. Cubic samples ($4 \times 4\,mm^3$) or bars ($4 \times 4 \times 25\,mm^3$) are sawn from the discs, for oxidation runs and mechanical tests, respectively.

2.3 Microstructure

The observation of rupture surfaces (SEM) or thin slices (TEM) shows a fine-grained microstructure (Figs 1 and 2). The whiskers, which do not dissolve in the liquid phase, hinder the intergranular diffusion and limit grain growth.[5] The distribution of the fibres is rather homogeneous with slight preferential orientation perpendicular to the pressing direction. To quantify this slight preferential orientation, Young's modulus was determined along the pressing direction ($E_{\parallel}$) and in the pressing plane ($E_{\perp}$). Young's modulus was calculated from the relation:

$$E = \rho(3V_L^2 - 4V_T^2/(V_L^2/V_T^2 - 1)$$

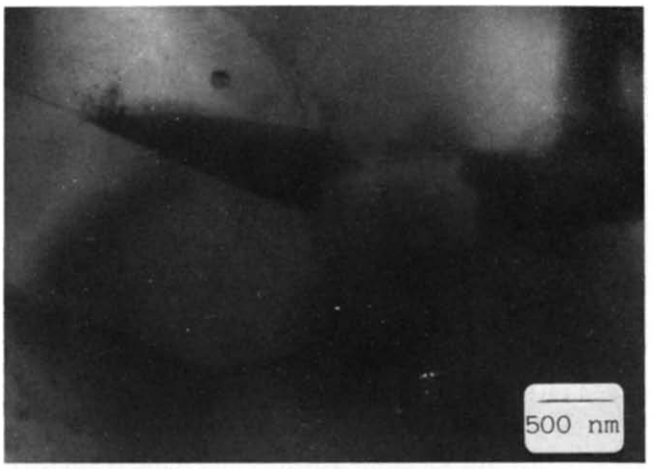

(a)

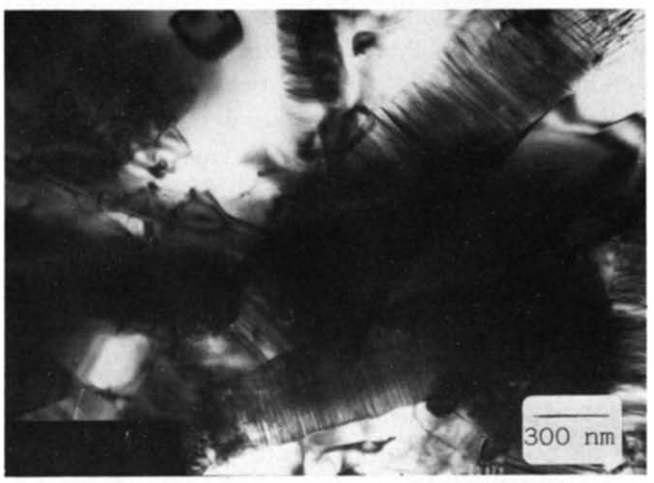

(b)

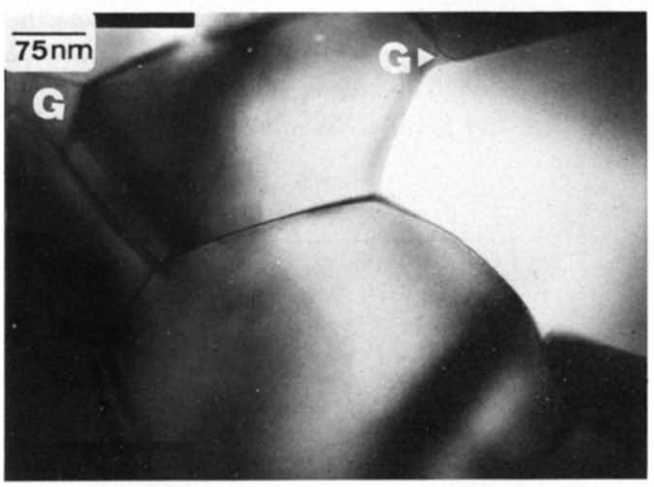

(c)

Fig. 2. TEM. (a) and (b) $SiC_w/SiAlYON$; (c) SiC_w/Si_3N_4–MgO.

where ρ is the density, V_L and V_T the velocities of longitudinal and shear ultrasonic waves. The ultrasonic velocities were measured using pulse-echo overlap techniques[6] with an accuracy better than 10^{-3}. A set of three measurements (along the pressing direction and two perpendicular directions in the pressing plane) was performed on the same sample to avoid density discrepancy. Results are presented in Table 1. The accuracy of the velocities and Young's modulus are respectively ± 10 m/s and ± 2 GPa.

Table 1. Young's modulus of SiC_w/Si_3N_4–MgO composites

Direction	*Pressing axis*	*Pressing plane*	
V_L, m/s	11 098	11 400	11 400
V_T, m/s	6 795	6 593	6 600
E, GPa	348	340	340

It must be noted that the presence of 30% SiC_w increases Young's modulus by 20% ($E_{Si_3N_4} = 280$ GPa). However whisker 'nests' are sometimes observed (Fig. 2(b)). The initial length of the fibres is reduced during the different stages of the fabrication but remains larger (5–10 μm) than the matrix grain size. Composites densified with MgO have a low quantity of glassy phase mainly located at triple point junctions. Very thin intergranular films may exist between grains (Fig. 2(c)). By contrast, the series containing yttria have a rather large amount of vitreous phase (Fig. 2(a)).

3 Oxidation Resistance

3.1 General features

The samples are oxidized in air during isothermal runs between 1300–1500°C (Fig. 3) using thermogravimetric equipment (Setaram B60). The frac-

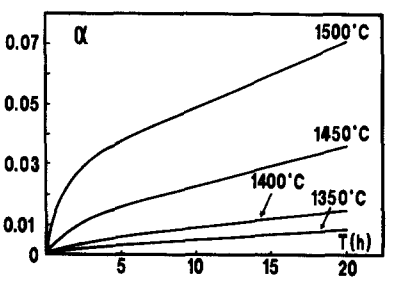

(a)

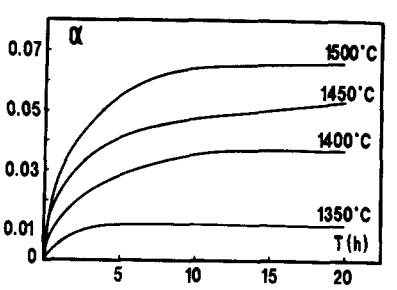

(b)

Fig. 3. Fractional weight gain versus time. (a) $SiC_w/SiAlYON$; (b) SiC_w/Si_3N_4–MgO.

tional weight gain α is defined by $\alpha = \Delta w_t / \Delta w_\infty$, where Δw_t is the weight gain at time t and Δw_∞ is the weight gain for a complete oxidation. Δw_∞ is deduced from the composition of the starting powders and the following reactions:

$$Si_3N_4 + 3O_2 \longrightarrow 3SiO_2 + \overrightarrow{2N_2}$$

$$SiC + 3/2O_2 \longrightarrow SiO_2 + \overrightarrow{CO}$$

Oxidation starts around 1350°C and becomes faster above 1400°C. The behaviour depends on the nature of the matrix. At the beginning the curves have a parabolic shape for both composites. Then, the reaction seems to stop in the case of the Si_3N_4–MgO matrix, whereas it goes on for the other matrix. Nevertheless, the oxidation remains slow even at 1500°C.

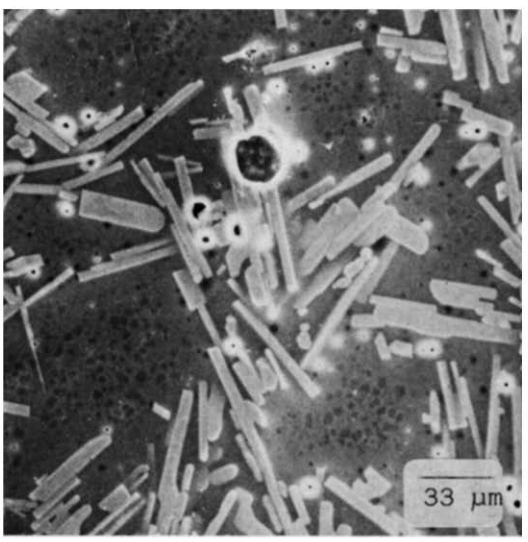

(a)

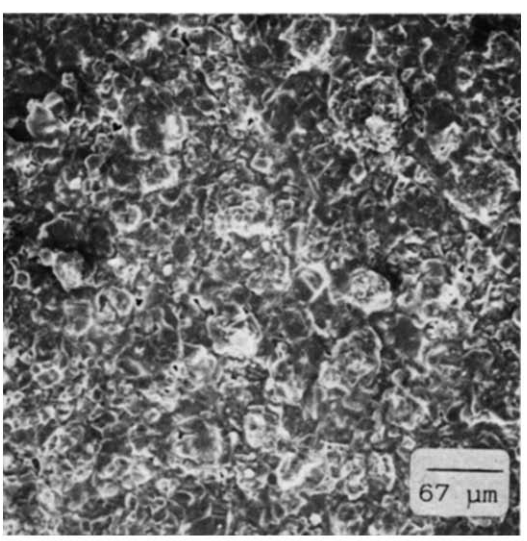

(b)

Fig. 4. SEM of composites oxidized at 1400°C. (a) SiC_w/SiAlYON; (b) SiC_w/Si_3N_4–MgO.

For SiC_w/SiAlYON composites oxidized at 1400°C the oxide scale consists of silica (SiO_2, α-cristobalite), yttrium silicate (δ-$Y_2Si_2O_7$) embedded in a vitreous silicate (Fig. 4). On polished cross-sections of samples exposed for 24 h, a colour change is noticed under the superficial oxide film. The depth of this zone increases as the reaction proceeds. This colour change reveals a preferential oxidation of the intergranular phase.[7] At 1450°C and above, the scale is thicker and becomes progressively porous.

For SiC_w/Si_3N_4–MgO composites, magnesium silicate ($MgSiO_3$) is detected instead of yttrium silicate, together with silica and a silicate glass at 1350°C. At higher temperatures, the scale is slightly porous. Microcracks appear during cooling, due to a more severe mismatch in this case between the expansion coefficients of the scale and the substrate.

The distribution of the metallic elements is determined by X-ray microanalysis on polished sections as a function of depth. The concentration profiles are presented in Fig. 5. Three regions can be distinguished:

(i) A very thin film, where the yttrium and calcium contents for SiC_w/SiAlYON are high (respectively magnesium and calcium for SiC_w/Si_3N_4–MgO);
(ii) a zone depleted in these metallic cations;
(iii) the unaffected substrate where the compositions are the original ones.

In the case of the SiC_w/SiAlYON composite the aluminium content remains constant through the whole section. This cation, which is essentially located in the β′-SiAlON solid solution, does not migrate.

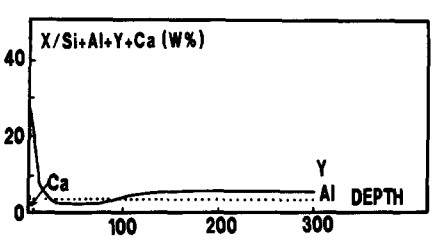

(a)

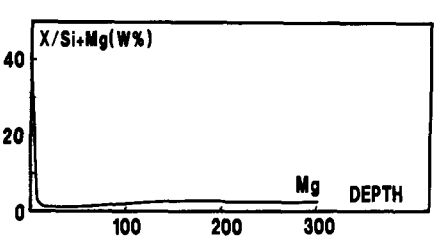

(b)

Fig. 5. Concentration profiles of metallic elements. (a) SiC_w/SiAlYON; (b) SiC_w/Si_3N_4–MgO.

3.2 Discussion

In the temperature range studied the reaction is very slow ($\alpha < 0{\cdot}07$ for 24 h). The decrease of the surface area at the internal interface can be neglected. Therefore it is possible to use the evolution of the fractional weight gain to study the kinetics.

The fractional weight gain curves have shapes similar to those observed for the oxidation of fluxed silicon nitride based ceramics.[7] The linearity of the curves $\alpha^2 = K_D t$ (Fig. 6) at the beginning of the plots shows that the reaction is initially controlled by a diffusional mechanism. The duration of this stage depends on temperature and matrix composition.

3.2.1 SiC_w/SiAlYON

For temperatures lower than 1450°C, the kinetics obey a diffusional process for the whole isothermal soaking time. The species migrate across the oxide film, which is protective. The viscosity of the coating decreases with rising temperature and with the accumulation of metallic impurities which are modifying cations. At 1500°C the change in the mechanism after a few hours seems to be a consequence of these two phenomena. The scale becomes more and more fluid. Molecular nitrogen formed at the internal interface escapes through this liquid, creating bubbles. The stirring of oxide scale facilitates the access of oxygen to the internal interface.

3.2.2 SiC_w/Si_3N_4–MgO

Whatever the temperature, the regime is diffusional during the first five hours. Then the reaction stops.

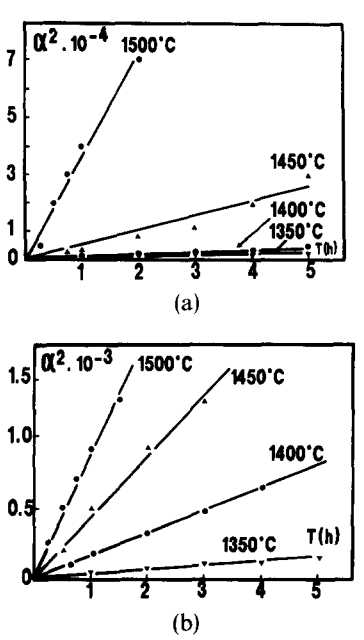

Fig. 6. Parabolic plots of fractional weight gain. (a) SiC_w/SiAlYON; (b) SiC_w/Si_3N_4–MgO.

This can be due to the very low quantity of vitreous phase. The narrowness of the intergranular films hinders the migration of the species.

The diffusion constants verify an Arrhenius law in all the temperature range, that allows the determination of the apparent activation energies ($E_{SiC_w/SiAlYON} = 800 \pm 30$ kJ/mol; $E_{SiC_w/Si_3N_4-MgO} = 520 \pm 20$ kJ/mol. These values are slightly higher than those calculated for the monolithic counterparts.[7,8] It is well known that the intrinsic oxidation resistance of both silicon nitride and silicon carbide are similar.[9] So it seems that the behaviour in air of the composites is controlled by the reactivity of the secondary nitrogen phases and their distribution. For the Si_3N_4–MgO matrix, the vitreous phase is mainly located in pockets poorly interconnected (Fig. 2(c)) and the reaction is quickly inhibited. In contrast, the secondary phase forms a continuous medium (Fig. 2(a)) in SiAlYON matrix composites, allowing the reaction to proceed.

4 Strength

4.1 Influence of the test temperature

The evolution of the mechanical strength with increasing temperature is studied in air. The bars are tested in three-point bending with a span of 20 mm. The heating rate is 50°C/min. The samples are maintained for 0·5 h at a constant temperature before testing to allow thermal equilibration. The loading rate is 0·2 mm/min. The modulus of rupture is reported in Fig. 7. It remains constant up to 1200–1300°C, then decreases rapidly. The behaviour is brittle up to 1200°C. Above this temperature, the intergranular phase softens and a plastic domain appears on the stress–strain curves. In the case of the composites, whisker pull out appears more and more on the fracture surfaces as the binding force between

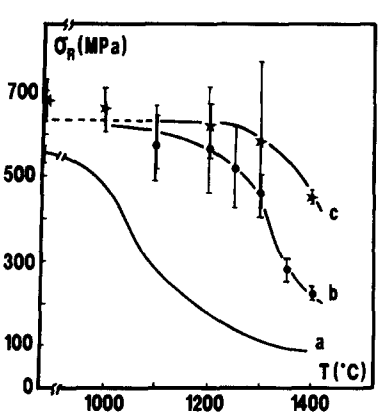

Fig. 7. Influence of temperature on the mechanical strength. a, SiAlYON; b, SiC_w/SiAlYON; c, SiC_w/Si_3N_4–MgO.

whiskers and matrix decreases (Fig. 8). The composite ceramics are more resistant than the monolithic at high temperatures, because of the bridging of the matrix grains by SiC whiskers impeding grain boundary sliding and slow crack growth. At 1300°C, the modulus of rupture of the SiC_w/SiAlYON composite is about 500 MPa, whereas that of its monolithic counterpart is about 120 MPa. The onset of the decrease in strength for the SiC_w/Si_3N_4–MgO is 100°C higher than for the SiAlYON matrix composite. The evolution in strength versus temperature depends on the refractoriness, but also on the amount of vitreous phase. Although ytrria and alumina lead to a more viscous glassy phase than magnesia, in the present case the very low quantity of MgO needed for full densification explains why the SiC_w/Si_3N_4–MgO composite exhibits the higher modulus of rupture.

4.2 Influence of oxidation on room-temperature strength

The influence of oxidation is studied in the 1100–1400°C temperature range. The samples are oxidized in air for 24 h then tested at room temperature (Fig. 9). When the temperature is lower than 1300°C, the oxidation products close the open porosity and heal the surface flaws. In the case of monolithic silicon nitride ceramics, an improvement of room-temperature strength is noted.[10] In contrast, for the composites, the strength is not modified by the thermal cycle, which implies that the critical flaw population is unaffected by oxidation. This suggests that fracture originates at internal defects such as whisker 'nests' rather than surface defects. Above 1400°C, a loss in strength is observed. The formation of large bubbles and pits in the oxide scale results in the development of a population of new defects more severe than the original ones. The behaviour is then controlled by the defects in the oxidized layer, as is the case for the monolithics in the same oxidation range.

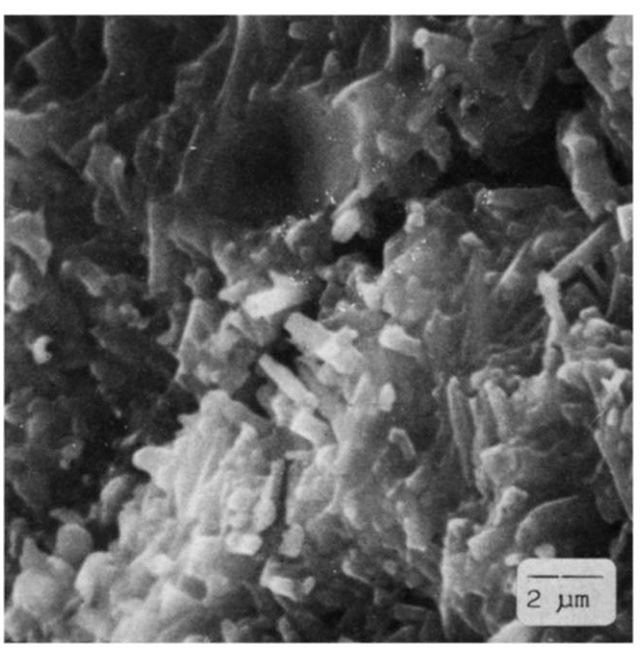

Fig. 8. SEM of a fracture surface: SiC_w/Si_3N_4–MgO.

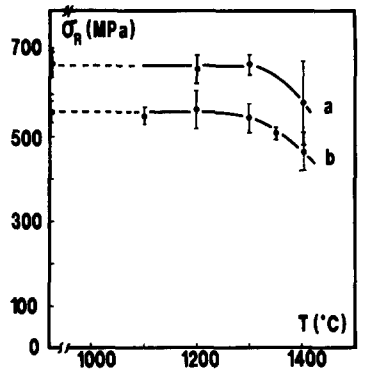

Fig. 9. Influence of oxidation on room-temperature strength. a, SiC_w/Si_3N_4–MgO; b, SiC_w/SiAlYON.

5 Creep

Creep behaviour is investigated in air between 1100 and 1300°C. The solicitation is the same as for the rupture tests. The stresses on the outer tensile fibre range from 100 to 300 MPa.

Creep curves are characterized by a long pseudo-stationary stage during which the creep rate diminishes slowly. The true steady state is reached only after 300 h as will be established below. The different materials were compared under the following test conditions: temperature 1200°C, stress 240 MPa, duration 60 h. For these test conditions, whatever the matrix, the higher the whisker content, the better the creep resistance (Fig. 10). For a given

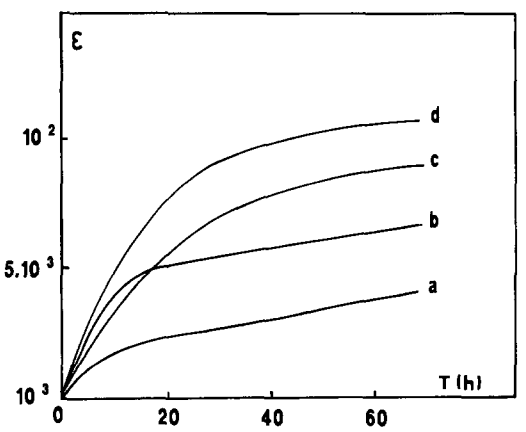

Fig. 10. Creep curves at 1200°C and 240 MPa. a, 30% SiC_w/66% Si_3N_4–4% MgO; b, 15% SiC_w/81% Si_3N_4–4% MgO; c, 30% SiC_w/70% SiAlYON; d, 15% SiC_w/85% SiAlYON.

whisker content, the SiAlYON matrix composites exhibit a lower creep resistance. This is likely to be the consequence of the large amount of glassy phase resulting from the high quantity of additives used for densification. Moreover, the raw materials have a rather high content in calcium impurity which segregates in the glassy phase, lowering its viscosity. However, it must be noted that at this temperature the flexural strength of the monolithic counterpart is lower than 200 MPa.

A more detailed study of the most resistant grade (SiC_w 30 vol.%/Si_3N_4–MgO) was undertaken to identify the mechanisms controlling deformation. The stress dependence and activation energy of the creep rate are derived from incremental stress changes at constant temperature (1200°C) and incremental temperature changes at constant stress (300 MPa) using the phenomenological relation:

$$\dot{\varepsilon} = f(s) \cdot \sigma^n \cdot \exp -(E/KT)$$

where σ is the applied stress, n the stress exponent, E the activation energy, K Boltzmann's constant, T the absolute temperature and $f(s)$ a function of the microstructure.

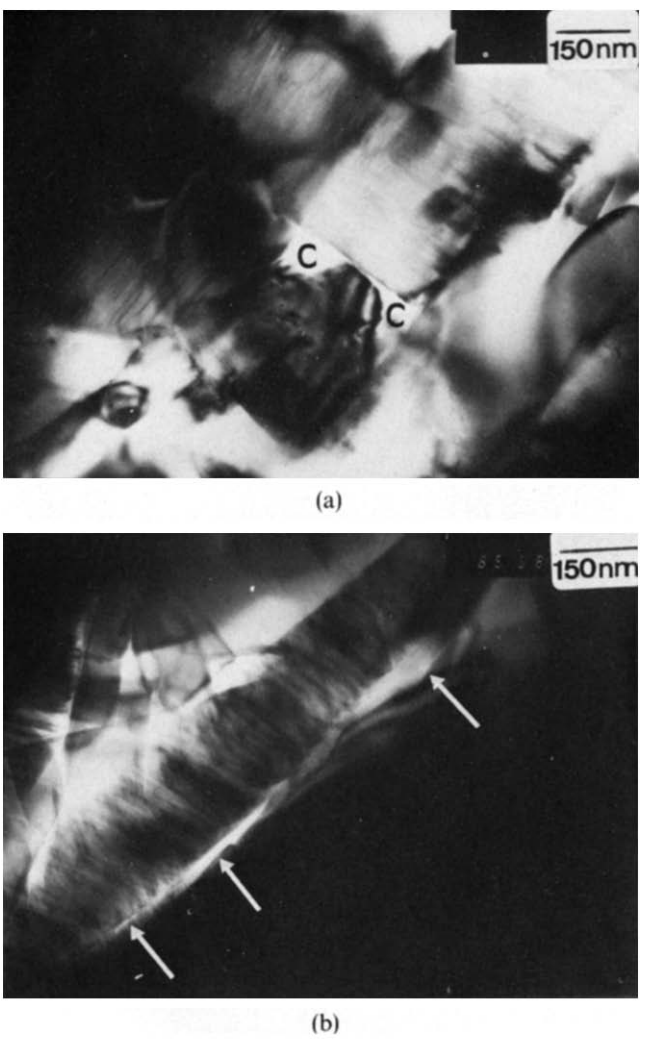

Fig. 11. TEM micrographs of crept samples. (a) Voids are indicated by C; (b) crack along a whisker boundary (arrowed).

In order to ascertain that the steady state has been reached, increasing and decreasing steps were performed until the same creep rate was measured for two non-consecutive steps corresponding to identical values for stress and temperature. This condition was satisfied after 300 h. The creep test lasted 600 h. The values derived from these experiments ($n = 3{\cdot}4$, $E \simeq 670$ kJ/mol) are consistent with those obtained at 1300°C by Backhaus-Ricoult *et al.*[11] for a similar composite crept in compression in a nitrogen atmosphere. The value of the stress exponent ($\neq 1$) excludes the possibility of creep being controlled by diffusional mechanisms. TEM investigations of the crept composites show the presence of large voids located at whisker tips and eventually extended microcracks along whisker–matrix grain interfaces (Fig. 11). Under the present experimental conditions, creep seems to be controlled by grain-boundary sliding. The enhanced creep resistance of the composites suggests that sliding is impeded by the SiC whiskers, the length of which remains, after processing, larger than the matrix grain size. This hindrance of sliding could, after long-term creep, account for the formation of voids and microcracks observed in the samples.

6 Conclusion

Different grades of silicon nitride based composites with SiC whiskers were prepared. The starting powders and the whiskers were mixed in a liquid medium. The slurries were filtered under a gas pressure and the green bodies densified by hot pressing.

The samples exhibit a good oxidation resistance up to 1400°C. The fractional weight gain depends on the volume and the composition of the intergranular phases as for monolithic materials. The incorporation of whiskers in a matrix does not alter the oxidation behaviour, whereas in the case of long-fibre SiC composites, the interphase between the fibre and the matrix provides a path for preferential oxidation.

Due to the presence of whiskers, grain-boundary sliding is restricted and high-temperature strength improved in comparison with non-reinforced materials. From the study of the room temperature strength of samples oxidized at increasing temperatures, it is concluded that the rupture is controlled by internal defects such as whisker nests. Improvements in processing lead to higher properties.

Creep resistance increases with whisker content. The deformation of the matrix is hindered by the whiskers which retain a high aspect ratio after sintering.

References

1. Wei, G. C. & Becher, P. F., Development of SiC-whisker reinforced ceramics. *Am. Ceram. Soc. Bull.*, **65** (1985) 298–304.
2. Buljan, S. T., Baldoni, J. G. & Huckabee, M. L., Si_3N_4–SiC composites. *Am. Ceram. Soc. Bull.*, **66** (1987) 347–52.
3. Nickel, K. G., Hoffmann, M. J., Greil, P. & Petzow, G., Thermodynamic calculations for the formation of SiC-whisker reinforced Si_3N_4 ceramics. *Adv. Ceram. Mat.*, **3** (1988) 557–62.
4. Debaig, C., Goursat, P. & Desmarres, J. M., European Patent 884003237, OEB: 0282 376; 14/8, 1988.
5. Buljan, S. T., Baldoni, J. G., Huckabee, M. L. & Zilberstein, G., Microstructure and fracture toughness of silicon nitride composites. *Proc. A.S.M.I.*, ed. R. A. Bradley, D. E. Clark, D. C. Larsen & J. O. Stiegler, 1988, pp. 113–23.
6. Papadakis, E. P., Ultrasonic phase velocity by pulse-echo-overlap method incorporating diffraction phase corrections. *J. Acoust. Soc. Amer.*, **42** (1967) 1045–51.
7. Bouarroudj, A., Goursat, P. & Besson, J. L., Oxidation resistance and creep behaviour of a silicon nitride ceramic densified with Y_2O_3. *J. Mat. Sci.*, **20** (1985) 1150–9.
8. Cubicciotti, D. & Lau, K. H., Kinetics of oxidation of hot pressed silicon nitride containing magnesia. *J. Am. Ceram. Soc.*, **61** (1978) 512–17.
9. Schlichtling, J., Oxygen transport through silica surface layers on silicon containing ceramic materials. *High Temperatures–High Pressures* **14** (1982) 717–24.
10. Goursat, P., Bouarroudj, A. & Besson, J. L., Influence of corrosion and microstructure on mechanical properties of SiYON ceramics. *Progress in Nitrogen Ceramics*, ed. F. L. Riley. Nijhoff, 1983, pp. 557–64.
11. Backhaus-Ricoult, M., Castaing, J. & Routbort, J. L., Creep of SiC-whisker reinforced Si_3N_4. *Revue Phys. Appl.*, **23** (1988) 239–49.